

Trade-off between vegetation CO₂ sequestration and fossil fuel-related CO₂ emissions: A case study of the Guangdong–Hong Kong–Macao Greater Bay Area of China

Zhaohui Luo^{a,b}, Yanyan Wu^c, Lixuan Zhou^{a,b}, Qiang Sun^a, Xijun Yu^{a,b}, Luping Zhu^{a,b}, Xiaojun Zhang^{a,b}, Qiaoli Fang^{a,b}, Xiao Yang^{a,b}, Jian Yang^a, Mingyi Liang^{a,b}, Hengjun Zhang^{a,*}

^a South China Institute of Environmental Sciences, Ministry of Ecology and Environmental, Guangzhou 510655, China

^b State Environmental Protection Key Laboratory of Urban Ecological Simulation and Protection, Guangzhou 510655, China

^c Guangdong University of Finance & Economics, Guangzhou 510655, China

ARTICLE INFO

Keywords:

Carbon dioxide emissions
Carbon budget
Nighttime light data
Carbon neutrality

ABSTRACT

Carbon neutrality has attracted tremendous attention. Cities contribute the most to CO₂ emissions. However, the contribution of vegetation to fossil-fuel-related CO₂ emissions in urban agglomeration is unclear. Clarifying the trade-off role of vegetation can disaggregate carbon reduction targets down to sub-units to adapt to and even mitigate global warming. In this study, the Guangdong–Hong Kong–Macao Greater Bay Area (GBA), one of the world's largest metropolitan areas, was studied using our proposed inter-calibration method. The results showed that the inter-calibration method is satisfactory and that the EANTLI model effectively decreases the blooming and saturation effects of nighttime light. In addition, fossil-fuel-related CO₂ emissions increased significantly ($P < 0.0001$) in the GBA during 2000–2018, while the variation in CO₂ sequestrations was far lower than that in the increase in emissions. CO₂ sequestrations by vegetation fully offset fossil-fuel-related CO₂ emissions in 2000, while the status reversed after 2001. Our findings illustrate the role of vegetation carbon sequestration in offsetting fossil-fuel-related CO₂ emissions and emphasize the importance of a CO₂ budget. Additionally, the *one city, one policy* strategy is a good choice for further adapting to and mitigating global warming.

As the global community is focusing on stabilizing the climate and keeping the global temperature increase within 1.5 °C in relation to pre-industrial levels (Wu et al., 2020), decreasing carbon emissions and carbon neutrality are attracting enormous attention. However, with the rapid economic growth in the past two decades, the demand for fossil-fuel-related energy has dramatically increased (Zhao et al., 2018), accounting for more than 70% of the total greenhouse gas emissions into the atmosphere (Meng et al., 2017) and becoming the largest factor accelerating global warming (Ou et al., 2015). In addition, the large amount of carbon dioxide (CO₂) emissions has had significant effects on biological, physical, and socioeconomic systems, such as urban heat islands, biodiversity loss, decline in agriculture productivity, and sea level rise (Coutts et al., 2010; Hirano & Yoshida, 2016). Therefore, understanding the status of CO₂ emissions and the capacity of vegetation to absorb CO₂ is considered a fundamental step in developing a CO₂

reduction strategy and achieving carbon neutrality.

China consumes 20% of the global primary energy and generates approximately a quarter of global CO₂ emissions, of which 85% are contributed by city energy usage (Shan et al., 2017). To mitigate the adverse effects of CO₂ emissions on ecosystems, the Chinese government has proposed to decrease CO₂ emissions to 60%–65% below 2005 levels by 2030 (Liu et al., 2020; Zhao et al., 2018), and encourage regions, where conditions permit, to take the lead in achieving a carbon peak and carbon neutrality; and achieved carbon neutrality before 2060. Therefore, the total CO₂ emissions and their spatial distribution are critical for policy-makers to consider when working toward emission reductions and monitoring in high-emission areas (Han et al., 2020b).

Cities are the main energy consumers and contribute 85% of the CO₂ emissions in China (Shan et al., 2017), playing a critical role in mitigating climate change (Yang & Li, 2013). Therefore, research on carbon emissions at the city scale requires further attention (Jiang et al., 2020; Liu et al., 2020; Zhou et al., 2021). In addition, an effective

* Corresponding author.

E-mail address: lzhzsdx@163.com (H. Zhang).

<https://doi.org/10.1016/j.scs.2021.103195>

Received 12 March 2021; Received in revised form 13 July 2021; Accepted 17 July 2021

Available online 21 July 2021

2210-6707/© 2021 Elsevier Ltd. All rights reserved.

understanding of the status of city-level CO₂ emissions is urgently required to develop an emission reduction policy and mitigate climate change. With the carbon neutrality goal in mind, it is essential to explore the CO₂ budget in city aggregation areas in order to allow for a robust carbon reduction and sequestration strategy (Wang & Cai, 2017) promoting local sustainability and addressing global climate change.

Many researchers have elucidated the CO₂ emissions of administrative units partly due to the limitations of fossil-fuel-related energy data statistics based either on energy balance table or sectoral energy consumption data or on point source carbon emission data (Gudipudi et al., 2019; Jing et al., 2018; Ribeiro et al., 2019). However, statistical data only provide numerical records of fossil-fuel-related energy consumption for an entire unit, and it is difficult to recognize high-emission hotspots in the unit (Su et al., 2014). To quantify the spatial pattern of CO₂ emissions, satellite data (e.g., the Open Source Data Inventory of Anthropogenic CO₂ Emission (ODIAC)) and other auxiliary data (e.g., nighttime light data) are extensively used with fine resolution. However, some limitations exist in relation to estimating the spatial patterns of CO₂ emissions based on nighttime light data. For example, the well-known blooming and saturation effects restrict the capacity of DMSP-OLS data to determine CO₂ emissions, while NPP-VIIRS data have high gain settings, incurring a lot of background noise (Shi et al., 2014). Additionally, NPP-VIIRS nighttime light data start only from 2012, while DMSP-OLS data are available only from 1992 to 2013. Therefore, it is necessary to combine DMSP-OLS and NPP-VIIRS data to estimate CO₂ emissions over a long time series (Shi et al., 2014). However, due to the difference between sensors and the divergent radiance ranges between DMSP-OLS and NPP-VIIRS nighttime light data, inter-calibration between them is difficult and has recently become one of the most eagerly awaited researches (Bennett & Smith, 2017; Zhao et al., 2019b). Moreover, CO₂ emissions based on nighttime light data are usually identified in lit areas, unlit areas with a high population density, or areas of extensive industrial activity, which can cause some CO₂ emissions to be ignored or impossible to estimate. In addition, the role of vegetation in CO₂ sequestration, which can offset energy-related CO₂ emissions, has been largely neglected, especially in urban agglomeration.

The Guangdong–Hong Kong–Macao Greater Bay Area (GBA) is an agglomeration of cities in China, which was established to strengthen international cooperation. However, there is insufficient literature of the spatial distribution of carbon emissions in the GBA (Lin & Li, 2020; Zhou et al., 2018), and the trade-off role of vegetation in fossil fuel CO₂ emission sequestration in the GBA.

In this study, the spatiotemporal variation of the CO₂ budget (the difference between CO₂ sequestration and CO₂ emissions) based on nighttime light data, fuel-related energy statistical data, and net primary productivity (NPP) were explored in the GBA based

T

deleted. Please check.

3.2. Dataset and methodology

3.2.1. Dataset

The dataset applied includes statistics on energy consumption, products of the moderate-resolution imaging spectroradiometer (MODIS) enhanced vegetation index (EVI), and MODIS yearly NPP, population density and nighttime light data (DMSP-OLS and NPP-VIIRS).

Fossil-fuel-related energy consumption data for estimating CO₂ emissions were acquired from the corresponding City Statistical Yearbooks and China Energy Statistical Yearbooks. Considering the availability and limitation of data at the city level, the energy consumption data were mostly statistical based on standard coal. Therefore, total CO₂ emissions in the GBA were calculated using the method proposed by Tu and Liu (2014).

Terra MODIS products, namely, MOD13A3 and MOD17A3H, were downloaded from the Land Processes Distributed Active Archive Center (LP DAAC). MOD13A3 is an EVI product with a temporal and spatial resolution of 1 month and 1 km, respectively, generated since 2000. The quality flag files were first referenced to exclude bad pixels, and the annual mean EVI was calculated to decrease the sensitivity of seasonal and inter-annual fluctuations (Zhang et al., 2013). Finally, pixels with an EVI value of less than 0 were removed to further mask non-vegetation.

the actual urban area based on the City Statistical Yearbook. DN_{max} and DN_{min} are the maximum and minimum values of nighttime light data, respectively; DN_i is the one-step value from DN_{max} to DN_{min} ; and ΔDN_i is the minimum difference between $DN_{total}^{DN_i}$ and S_{stats} for all step values from DN_{max} to DN_{min} .

A suitable threshold could be obtained at the point where Eq. (7) was satisfied. The area was divided into two parts according to the threshold, namely urban and rural. The rural area was further divided into a lit area (pixel values of nighttime light data are greater than 0) and an unlit area (pixel values of nighttime light data = 0).

(2) The urban and rural areas with nighttime lights were extracted as a mask to cover the population density grid, and the total population from the lit urban and lit rural areas, namely TP_{Lu} and TP_{Lr} , respectively, were extracted. The remaining part of the area was calculated similarly to obtain the total population in the unlit rural area, namely TP_{Unlr} .

(3) The total CO₂ emissions from the lit urban, lit rural, and unlit rural areas were estimated. The CO₂ emission per capita in the urban area is EPC_{urban} and the CO₂ emission per capita in the rural area is $EPC_{rural} \times x_i$, where x_i is the rural area:urban area ratio of CO₂ emissions per capita. This ratio is equal to 0.08068, 0.0780, 0.0795, and 0.1197 for 2000-2003, 2004-2007, 2008-2012, and 2013-2018, respectively based on the study by Liu et al. (2018) in Guangdong Province. Then, the total CO₂ emissions from the lit urban, lit rural, and unlit rural areas can be expressed as Equations (8)-(10):

$$CO_2^{LU} = EPC_{urban} \times TP_{Lu} \quad (8)$$

$$CO_2^{LR} = EPC_{rural} \times TP_{Lr} \quad (9)$$

$$CO_2^{ULR} = EPC_{rural} \times TP_{Unlr} \quad (10)$$

where CO_2^{LU} , CO_2^{LR} , and CO_2^{ULR} represent CO₂ emissions in the lit urban, lit rural, and unlit rural areas, respectively, and the unit for CO_2^{LU} , CO_2^{LR} , and CO_2^{ULR} is megaton (Mt).

Since the total CO₂ emissions were the sum of the lit urban, lit rural, and unlit rural areas (Equation (11)), EPC_{urban} was expressed as Eq. (12) according to Eqs. (8)-(11).

$$TCO_2 = CO_2^{LU} + CO_2^{LR} + CO_2^{ULR} \quad (11)$$

$$EPC_{urban} = \frac{CO_2^{LU}}{TP_{Lu}} \quad (12)$$

where TCO_2 is the total CO₂ emissions (Mt) in the study region.

(4) Finally, CO₂ emissions in the lit area at the pixel level were distributed in proportion to the values of adjusted nighttime light data mentioned above, while CO₂ emissions in the unlit area at the pixel level were distributed in proportion to the population counts (Eqs. (13)-(14)).

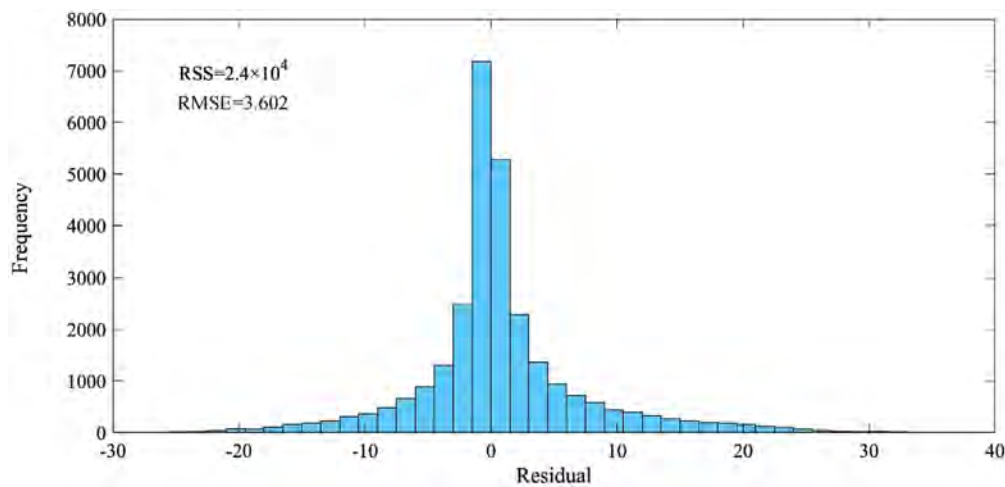
$$CO_2^{Li} = \frac{CO_2^{LU} + CO_2^{LR}}{Total_{lig}} \times Total_{pop} \times Lig_i \quad (13)$$

$$CO_2^{Uj} = \frac{CO_2^{ULR}}{Total_{pop}} \times pop_j \quad (14)$$

where CO_2^{Li} and CO_2^{Uj} represent CO₂ emissions in lit and unlit areas of pixel i and j , respectively (Mt); $Total_{lig}$ and $Total_{pop}$ represent total nighttime light values and total population values in the GBA, respectively; and Lig_i and pop_j represent nighttime light values of pixel i and population values of pixel j , respectively.

3.2.2.4. Trends in CO₂ emissions. The trend in CO₂ emissions during 2000-2018 at the pixel level was calculated based on robust non-parametric Mann-Kendall (M-K) and Theil-Sen median slope analysis, which could avoid autocorrelation in inter-annual time series data (Luo and Yu, 2017). Additionally, the trend in CO₂ emissions was also analyzed using the annual percentage change (APC) method. The APC is calculated as follows:

Scatter plot of the original NPP-VIIRS and DMSP-OLS pixel pairs (a), and a scatter plot of logarithmically transformed NPP-VIIRS and original DMSP-OLS pixel pairs (b) in corresponding radiation-stable areas. The red curves denote the fitted model.



Frequency distribution of the residual sum of squares between DMSP-OLS and estimated NPP-VIIRS for 2013 based on the logistical model.

Parameters of the logistical model

Model	a	b	c	d
Logistical model	4.315	60.851	0.275	3.742

approximately 0.867 Mt/a ($P < 0.0001$).

Fig. 5b details the spatial pattern of the temporal trend in mean annual CO₂ emissions. Over 19 years (2000-2018), more than 81.62% of the total pixels exhibited either significantly decreased or increased trends in the entire region. Areas with a decreased trend only accounted for 1.77% of the total area and mainly occurred in the northwest and northeast, with a decreasing rate of approximately -0.0005 to 0 Mt/km². However, more than 98% of the total region showed an increased trend, and approximately 81% had a significantly increased trend ($P < 0.05$), mainly distributed in the center and southeast, with an increasing rate greater than 0.001 Mt/km².

To validate the accuracy of the proposed model, a quantitative comparison was performed between the estimated data and actual statistical data. As the model allocated the actual statistical fossil-fuel-related energy of CO₂ emissions to the pixel level in the GBA, the estimated total CO₂ emissions in the GBA from 2000 to 2018 were re-aggregated and compared with the actual statistical data of each corresponding year. Additionally, the averaged CO₂ emissions of each city

from 2000 to 2018 were calculated and the total emissions aggregated and compared with the actual statistical data for the corresponding cities. The estimated and actual statistical data showed an almost linear relationship in the GBA, with R^2 , mean absolute error (MAE), and RMSE of 0.999, 0.046 Mt, and 0.106 Mt, respectively (Fig. 6a), indicating that CO₂ emissions in the GBA are neither underestimates nor overestimates. In addition, the estimated data at the city level showed a positive, linear relationship with actual statistical data, with an R^2 and mean relative error (MRE) of 0.8791 and 35.0796%, respectively (Fig. 6b). Indicating that the estimated model also performs well at the city scale despite being proposed at the regional scale.

4.3. Carbon sequestration by vegetation

Spatial patterns of the mean annual NPP and annual variation in the total NPP are displayed in Fig. 7. The mean annual NPP showed an increasing trend from the center to the sides. The lowest annual NPP ($< 0.579 \text{ kg}\cdot\text{C}/\text{m}^2$) was mainly distributed in the center and south, in which an impervious surface was mostly distributed under high urbanization. However, an NPP higher than $0.745 \text{ kg}\cdot\text{C}/\text{m}^2$ occurred in Hong Kong and Macao, which also have high urbanization. By contrast, the highest annual NPP ($> 1.236 \text{ kg}\cdot\text{C}/\text{m}^2$) mainly occurred in the northwest and northeast in areas with high vegetation coverage and relatively low urbanization, compared to Hong Kong or Macao. In terms of the

Latitudinal transects (23° N) of the original DMSP-OLS, VANUI, HIS, and EANTLI performed in the GBA (DMSP-OLS data of 2013 as an example).

temporal variation in the annual total NPP, we found a small fluctuation, with values ranging from 38.75 to 44.65 Mt. While the annual total NPP showed an increasing trend with a magnitude of approximately 0.03 Mt/a, the trend was not significant ($P = 0.664$).

4.4. Spatiotemporal patterns of the CO₂ budgets

Regarding the spatial patterns of the CO₂ budget, an increasing trend from the center to the sides can be observed, with three different levels (Fig. 8). The first level was lower than -0.020 Mt/km² and was mostly distributed in the center of the GBA. The second level ranged from -0.020 to 0 Mt/km² and was mainly distributed in the north of Foshan, Zhongshan, Zhuhai, Hong Kong, and Macao. The third level was greater than 0 Mt/km² and was only distributed in most parts of Zhaoqing, Jiangmen, and Huizhou. These results indicated that vegetation in these parts had the ability to fully absorb fossil-fuel-related CO₂ emissions during 2000-2018.

The temporal patterns of the total CO₂ budget displayed a significantly decreasing trend over the study period, with a magnitude of approximately -19.7 Mt/a ($P < 0.0001$). Vegetation in the GBA played a critical role in absorbing fossil-fuel-related CO₂ emissions and could fully offset these emissions in 2000. However, the CO₂ budget changed from positive to negative after 2000 as fossil-fuel-related CO₂ emissions significantly increased (0.867 Mt/a; Fig. 5a), while the NPP increased

non-significantly (0.03 Mt/a; Fig. 7) after 2000.

Fig. 9 depicts the CO₂ budget at the city level and shows that CO₂ budgets in Macao, Dongguan, Foshan, Shenzhen, Zhongshan, Zhuhai, Guangzhou, and Hong Kong were all negative from 2000 to 2018. The magnitudes of the CO₂ budget in Guangzhou and Zhuhai showed a continuous downward trend, and the absolute magnitudes of the CO₂ budget became even larger after 2013. By contrast, the negative magnitudes of the CO₂ budget in Dongguan, Foshan, Zhongshan and Shenzhen were mitigated after 2013, indicating the CO₂ sequestration by vegetation cannot fully offset fossil-fuel-related CO₂ emissions in these cities, especially Guangzhou and Zhuhai. For Huizhou and Jiangmen, the CO₂ budget changed from positive to negative value, and the turning point occurred in 2014, indicating that vegetation could fully offset fossil-fuel-related CO₂ emissions in Huizhou and Jiangmen during 2000-2013. However, the status could not be maintained after 2014. The CO₂ budget in Zhaoqing was positive during 2000-2018, indicating that vegetation in Zhaoqing could fully offset fixed-fossil fuel-related CO₂ emissions during the study period. However, this situation is not positive, as the CO₂ budget showed a downward fluctuating trend.

Spatial distribution and annual variation of CO₂ emissions in the GBA between 2000 and 2018. The top-right panel in represents the dynamics of the total CO₂ emissions from fuel consumption, and the red line indicates the linear fitting. The top-right panel in represents the count distributions of the mean annual variation in CO₂ emissions, and the values in parentheses indicate the percentage of pixels with significant trends ($P < 0.05$).

Comparison of estimated CO₂ emissions and actual statistical CO₂ emissions. (a) Total fossil fuel related-energy CO₂ emissions of 2000-2018 in the GBA and (b) mean fossil fuel related-energy CO₂ emissions of 2000-2018 for 11 cities.

5.1. Process of nighttime light data

Previous studies have tried to explore the relationship between DMSP-OLS and NPP-VIIRS. Li et al. (2017) applied a power function and convolution to perform an inter-calibration between DMSP-OLS and NPP-VIIRS, and the RMSE was 4.997. Jeswani et al. (2019) applied a logarithm and linear function, and the R^2 was 0.775. Wu and Wang (2019) used a power function and convolution in Beijing and Yiwu, and acquired an RMSE of 9.387 and 7.687, respectively. Ma et al. (2020) compared the linear function, logistical, and BiDoseResp models, and R^2 was 0.847, 0.967 and 0.967, respectively, and the RMSE was 2.847×10^6 , 6.199×10^5 , and 6.136×10^5 , respectively. They concluded that the BiDoseResp model is the best one. Compared with previous studies, our logistical function model in this study is better than the others based on the R^2 and the RMSE.

Light saturation effects limit the correlation between nighttime light

data and the estimation of CO₂ emissions and increase the uncertainty in CO₂ emission modeling. Unfortunately, previous studies (Lv et al., 2020; Shi et al., 2016; Su et al., 2014; Wang & Liu, 2017; Wang et al., 2019; Zhao et al., 2019a) have ignored the effects of saturation on nighttime light data during CO₂ emission modeling. Zhang et al. (2013) compared the HSI and the VANUI models to decrease the impacts of saturation on nighttime light data and concluded that the VANUI model significantly decreases the saturation of nighttime light data and is better than the HSI model. Zhao et al. (2018) compared three models (HSI, VANUI, and EANTLI) to reduce the saturation of nighttime light data, and the adjusted R^2 was 0.7102, 0.7548, and 0.7564 for HSI, VANUI, and EANTLI models, respectively, indicating that the VANUI model is better than the HSI model, consistent with Zhang et al. (2013). However, when compared with the EANTLI model, the R^2 of the VANUI model was lower, indicating that the EANTLI model is better in decreasing saturation effects, consistent with Liu et al. (2018), who showed that the EANTLI model is more suitable for CO₂ emission applications than the HSI and VANUI models. Similarly, our results showed that the EANTLI

Spatial pattern of the mean annual NPP during 2000-2018. Inset shows the annual variation in the total NPP in the GBA.

model is better than the other two models in alleviating the saturation problem in both urban and rural areas, which supports the conclusion of previous studies (Liu et al., 2018; Zhao et al., 2018; Zhou et al., 2015).

5.2. CO₂ emissions and sequestration

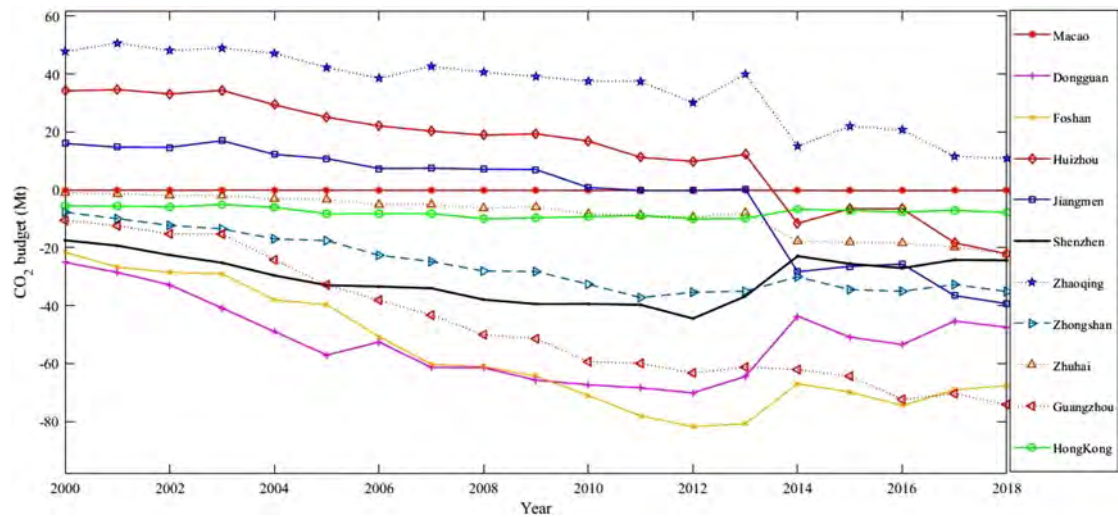
In this study, we estimated the CO₂ budget in the GBA as the difference between the NPP and fossil-fuel-related CO₂ emissions. With regard to CO₂ emissions, nighttime light data were combined with population data in order to overcome the issue that CO₂ emissions in unlit areas cannot be estimated based only on nighttime light data. We allocated the actual statistical fossil-fuel-related energy of CO₂ emissions to the pixel level, and to validate the result, we compared estimated and actual statistical data at both the regional and the city scale. The estimated and actual statistical data had an almost linear relationship, with the R^2 , the MAE, and the RMSE all being satisfactory at the regional scale due to the reason that we allocated the actual statistical fossil-fuel-related energy of CO₂ emissions. Although the R^2 reached 0.999 at the

regional scale, and was higher than that achieved by Ghosh et al. (2010), it was a little lower than that achieved by of Liu et al. (2018), which was 1. In terms of validation at the city scale, R^2 and the MRE were 0.8791 and 35.0796%, respectively. Ou et al. (2015) compared actual statistical data with three different emission maps (from NPP-VIIRS and population data, from RCP-DMSP-OLS and population data, and from SLP-DMSP-OLS and population data), and R^2 and the MRE were 0.8695, 0.8386, and 0.7590 and 36.31%, 40.29%, and 52.14%, respectively. Additionally, they compared actual statistical data with three different types of nighttime light data (NPP-VIIRS, RCP-DMSP-OLS, and SLP-DMSP-OLS), and the R^2 and the MRE were 0.8623, 0.8212, and 0.7628 and 36.98%, 41.27%, 52.31%, respectively. Liu et al. (2018) compared estimated and actual statistical emissions based on EANTLI and DMSP-OLS models, respectively, and R^2 value and the MRE were 0.8833 and 0.8182 and 37.92% and 52.35%, respectively. Our evaluation criteria of R^2 and the MRE were better than those of Ou et al. (2015). Although R^2 achieved by of Liu et al. (2018) was a little higher than that of ours, our MRE was lower than that of Liu et al. (2018).

Spatial pattern of the mean CO₂ budget during 2000-2018. Inset shows the annual variation in the total CO₂ budget in the GBA.

With regard to the spatial distribution of CO₂ emissions, high CO₂ emissions were mainly distributed in urban areas, while lower CO₂ emissions mainly occurred in sub-urban or rural areas, which is consistent with the spatial pattern of economic development and is similar to previous studies (Chuai & Feng, 2019; Wang et al., 2018). At city level, high CO₂ emissions mainly occurred in Guangzhou, Dongguan, and Shenzhen, which are developed or manufacturing cities with an intensive population density or energy consumption. The CO₂ emissions in Guangzhou were 100.45 Mt in 2005 and increased to 132.97 Mt in 2013. Wang et al. (2018) reported that Guangzhou, Dongguan, and Shenzhen had the highest CO₂ emissions in the Pearl River Delta, and CO₂ emissions in Guangzhou increased approximately from 93.45 Mt in 2005 to 127.44 Mt in 2013, similar to our results. Lin and Li (2020) found that CO₂ emissions in Shenzhen and Dongguan were 26.86 and 38.68 Mt, respectively, in 2017, similar to our estimates (27.92 and 49.0

Mt for Shenzhen and Dongguan, respectively). In addition, lower CO₂ emissions were dominant in Zhaoqing, Jiangmen, and north Huizhou, consistent with the result of Wang et al. (2018), and the reason may be the terrain being dominated by mountains and hills and the relatively low economic development level but high vegetation coverage. A significantly increasing temporal trend was found in CO₂ emissions, consistent with Wang et al. (2018), who concluded that most of the Pearl River Delta cities have had a rapid increase in CO₂ emissions in recent decades. Additionally, the high increase mainly occurred in developed areas, indicating that fossil-fuel-related energies were increasingly consumed in developed areas, despite the fact that these areas already have high CO₂ emissions. Moreover, we compared our results with CEADs dataset from 2000-2017 at the city scale (Fig. 10), and result show that the R², RMSE and MAE were 0.75, 6.20 Mt and 4.66 Mt, respectively.



Temporal trend in the CO₂ budget at the city level in the GBA during 2000-2018.

Comparison of CO₂ emissions between estimated data and CEADs data.

In terms of CO₂ sequestration, the spatial patterns of the NPP with lower values occurred mainly in urban areas and higher values were principally distributed in rural areas. The reason may be anthropogenic activities and the distribution of vegetation coverage. In rural areas, the intensity of development activities or human disturbance is low, favoring vegetation growth and resulting in high vegetation biomass and productivity. In contrast, in urban areas, the effects of disturbance, such as land use and land cover change in ecosystems and soil, are intensive, restraining vegetation growth (Meng et al., 2014).

With regard to CO₂ budgeting at the regional scale, CO₂ sequestration by vegetation could fully offset fossil-fuel-related CO₂ emissions in the GBA in 2000. However, the status could not be maintained at the beginning of 2001, indicating that fossil-fuel-related CO₂ emissions are more than CO₂ sequestration by vegetation, and the absolute difference between CO₂ sequestration by vegetation and fossil-fuel-related CO₂ emissions becomes increasingly larger over the years. The reason is that the majority of CO₂ emissions come from energy consumption and result in a significantly increased trend in CO₂ emissions. However, the NPP increased at a non-significant rate, and the magnitude of NPP variation

was much lower than that of CO₂ emissions, indicating that CO₂ sequestration by vegetation alone is not enough to achieve carbon neutrality and the reduction in CO₂ emissions seems more critical CO₂ sequestration by vegetation in the GBA.

CO₂ budgeting at the city scale was a little different from that at the regional scale. CO₂ sequestration by vegetation could not offset fossil-fuel-related CO₂ emissions in Macao, Dongguan, Foshan, Shenzhen, Zhongshan, Zhuhai, Guangzhou, and Hongkong during the study period (2000-2018), while in Huizhou and Jiangmen, vegetation could fully absorb fossil-fuel-related CO₂ emissions during 2000-2013, but the CO₂ budget in Huizhou and Jiangmen became negative during 2014-2018. The CO₂ budget in Zhaoqing was positive during 2000-2018, indicating that vegetation could fully offset fossil-fuel-related CO₂ emissions during the study period. However, this situation is not positive in Zhaoqing due to the downward fluctuating trend in the CO₂ budget. The discrepancy in the CO₂ budget between cities may be due to the difference in economic development that results in different fossil-fuel-related energy consumption and divergent land use and land cover change (Luo et al., 2018b; Wang et al., 2018). These discrepancies

significantly affect both CO₂ emissions and CO₂ sequestration by vegetation. Our results can not only improve our understanding of the spatiotemporal variation in CO₂ emissions, but also offer a reference to allocating CO₂ reduction targets down to each city. Therefore, scientists and government decision makers should pay more attention to the *one city, one policy* strategy to create a CO₂ balance between CO₂ sequestration and CO₂ emissions, especially in the core area of the GBA, such as Guangzhou, Foshan, Dongguan, and Shenzhen, with high CO₂ emissions and low CO₂ sequestration. In addition, focus should be on the CO₂ budget in Zhaoqing, and more efforts such as afforestation, to increase the NPP, and more measures such as renewable energy promotion and application, to decrease fossil-fuel-related CO₂ emissions, should be emphasized to slow down the positive–negative trend in the CO₂ budget.

5.3. Policy implications

Environmental policy formulation cannot be made solely based on CO₂ emissions, but the net CO₂ emissions should also be considered. Therefore, several policy recommendations to decrease CO₂ emissions and increase CO₂ sequestration were proposed.

First, considering the spatiotemporal dynamics of CO₂ emissions in the GBA, a model based on nighttime light data should be established at a regional-city-county scale to provide reliable and refined data. Additionally, a mechanism to decrease CO₂ emissions should be established in regions with high CO₂ emissions, especially in the Pearl River Delta region.

ri

This work was supported by Science and Technology Program of Guangzhou, China (No.201904010288), the National Science Foundation of China (NO.42001214), and Central Fund Supporting Nonprofit Scientific Institutes for Basic Research and Development (No. PM-zx703-201904-139).

Supplementary material associated with this article can be found, in the online version, at [doi:10.1016/j.scs.2021.103195](https://doi.org/10.1016/j.scs.2021.103195).

- Bennett, M. M., & Smith, L. C. (2017). Advances in using multitemporal night-time lights satellite imagery to detect, estimate, and monitor socioeconomic dynamics. *Remote Sensing of Environment*, *192*, 176–197.
- Cai, B., et al. (2018). China high resolution emission database (CHRED) with point emission sources, gridded emission data, and supplementary socioeconomic data. *Resources, Conservation and Recycling*, *129*, 232–239.
- Cao, Z., Wu, Z., Kuang, Y., & Huang, N. (2015). Correction of DMSP/OLS Night-time Light Images and Its Application in China. *Journal of Geo-information Science*, *17*(9), 1092–1102.
- Chen, J., Zhao, F., Zeng, N., & Oda, T. (2020a). Comparing a global high-resolution downscaled fossil fuel CO₂ emission dataset to local inventory-based estimates over 14 global cities. *Carbon Balance Manag.* *15*(1), 9.
- Chen, Y., et al. (2020b). Relationships of ozone formation sensitivity with precursors emissions, meteorology and land use types, in Guangdong-Hong Kong-Macao Greater Bay Area, China. *Journal of Environmental Sciences*, *94*, 1–13.
- Chuai, X., & Feng, J. (2019). High resolution carbon emissions simulation and spatial heterogeneity analysis based on big data in Nanjing City. *China. Science of The Total Environment*, *686*, 828–837.
- Coutts, A., Beringer, J., & Tapper, N. (2010). Changing Urban Climate and CO₂ Emissions: Implications for the Development of Policies for Sustainable Cities. *Urban Policy and Research*, *28*(1), 27–47.
- Ghosh, T., et al. (2010). Creating a Global Grid of Distributed Fossil Fuel CO₂ Emissions from Nighttime Satellite Imagery. *Energies*, *3*(12), 1895–1913.
- Gocic, M., & Trajkovic, S. (2013). Analysis of changes in meteorological variables using Mann-Kendall and Sen's slope estimator statistical tests in Serbia. *Global and Planetary Change*, *100*, 172–182.
- Gudipudi, R., et al. (2019). The efficient, the intensive, and the productive: Insights from urban Kaya scaling. *Applied Energy*, *236*, 155–162.
- Han, J., et al. (2017). A long-term analysis of urbanization process, landscape change, and carbon sources and sinks: A case study in China

- Zhou, L., Zhang, X., Zheng, J., Tao, H., & Guo, Y. (2015). An EVI-based method to reduce saturation of DMSP/OLS nighttime light data. *Acta Geographica Sinica*, 70, 1339–1350.
- Zhou, Y., Chen, M., Tang, Z., & Mei, Z. (2021). Urbanization, land use change, and carbon emissions: Quantitative assessments for city-level carbon emissions in Beijing-Tianjin-Hebei region. *Sustainable Cities and Society*, 66, Article 102701.

- Zhou, Y., Shan, Y., Liu, G., & Guan, D. (2018). Emissions and low-carbon development in Guangdong-Hong Kong-Macao Greater Bay Area cities and their surroundings. *Applied Energy*, 228, 1683–1692.